ELSEVIER

Thermochimica Acta 324 (1998) 203–213

thermochimica acta

Thermal behavior of asphalt cements

P.M. Claudy[a,*], J.M. Létoffé[a], D. Martin[b], J.P. Planche[b]

[a] *CNRS, Laboratoire des Matériaux Organiques à Propriétés Spécifiques BP 24, 69390 Vernaison, France*
[b] *Centre de Recherche ELF de Solaize BP 22, 69360 Vernaison, France*

Abstract

Asphalt cements are highly complex mixtures of hydrocarbon molecules whose thermal behavior is of prime importance for petroleum and road industry.

From DSC, the determination of several thermal properties of asphalts is given, e.g. glass-transition temperature and crystallized fraction content.

The dissolution of a pure *n*-paraffin C_nH_{2n+2} in an asphalt, as seen by DSC, should be a single peak. For $20<n<32$ two peaks were observed. This means that their dissolution occurs in two liquids, and explains the usual shape of the DSC traces of AC, which shows a minimum at 35° to 40°C.

At room temperature, an asphalt cement is a mixture of two liquids containing some crystallized fractions. Above 80°C, it appears as a single liquid phase. At low temperature, the study of the glasses formed was done, using either constant or variable heating rate DSC. This technique, shows two glass transitions, for an asphalt containing a high quantity of crystallized fractions. The T_g of these glasses change with time and temperature. The formation of the crystallized phases is superposed to the enthalpic relaxation of the glasses, making a kinetic study very difficult.

Keywords: Analysis; Asphalt cements; Glass transition; Liquid–liquid demixtion; Relaxation

1. Introduction

Asphalt cements (AC) are highly complex mixtures of a large number of different chemical species. Their structure and properties are highly temperature dependent, as reported in Mack's compilation of literature [1]. Previous study of their thermal behavior primarily consisted in attempts to correlate their glass-transition temperature with their asphaltene or paraffin content [2], or more recently, to link their glass-transition temperature to their molecular size and composition. Noël and Corbett [3] pioneered the study of AC thermal characteristics over a broad range of temperature. They were interested in in-situ crystallization and the thermal effects observed in fractions extracted by precipitation and separation by chromatographic methods. It was also shown that the thermal behavior of AC is greatly influenced by its thermal past. Differential scanning calorimetry (DSC) was used to directly evaluate crystallized fractions in AC [4]. The authors attempted to correlate the DSC results with those obtained using a normalized procedure (NFT 66-015). A quantitative study of the thermal behavior of AC under an inert atmosphere was carried out by DSC to identify the asphalt fractions responsible for the crystallization and to develop a quantitative thermoanalytical method. The next step was to measure the crystallization and the dissolution of these fractions as a function of temperature and try to correlate these results and the AC physical properties. Very recently, as a part of their work for the Strategic Highway Research Program (SHRP), Anderson et al.

*Corresponding author.

0040-6031/98/$ – see front matter
PII: S0040-6031(98)00537-1

[5] reported an important phenomenon in AC, which they defined as 'low temperature physical hardening'. This effect was related to a gradual density change depending on time and temperature (−15°C). DSC and thermomicroscopy experiments were simultaneously used to relate the change in AC structure and their rheological properties.

2. DSC, thermodynamics and kinetics

In thermoanalytical methods, temperature is a function of time. The behavior of the system under study, is a complex function of time and temperature, given by kinetics and thermodynamics: the kinetics say how fast the thermodynamic equilibrium will be reached. The use of DSC makes the problem difficult, because the measurement gives the sum of the heat capacity of the system, and the heat effect occurring in the sample.

It seemed useful to go back to the fundamental equations to understand the significance of the data, especially on using non-linear heating rate.

2.1. Thermodynamics

The enthalpy of a system, is a function of a number of independent variables, which are usually not known and even difficult to establish. It was shown [6] that the most general thermodynamic description of a system requires at least three variables. Enthalpy H of a system, made of one unit of a pure compound, is given by $H(T, P, \xi)$. Using Prigogine's notations [6], ξ is the degree of advance of some transformation occurring in the system and its enthalpy change is $\Delta_r H$. The total differential of H is:

$$\frac{dH}{dT} = \left(\frac{\partial H}{\partial T}\right)_{P,\xi} + \left(\frac{\partial H}{\partial P}\right)_{T,\xi}\frac{dP}{dT} + \left(\frac{\partial H}{\partial \xi}\right)_{T,P}\frac{d\xi}{dT} \tag{1}$$

By definition $C_p = dH/dT$ and $C_{p\xi} = (\partial H/\partial T)_{P,\xi}$ and $\Delta_r H = (\partial H/\partial \xi)_{T,P}$. C_p is sometime refereed to as 'apparent heat capacity', $C_{p\xi}$ is called the 'true heat capacity', and the configurational heat capacity C_p (conf) is given by

$$C_p(\text{conf}) = \left(\frac{\partial H}{\partial \xi}\right)_{T,P}\frac{d\xi}{dT} = \Delta_r H\frac{d\xi}{dT}$$

2.2. Kinetics

At a constant pressure, the power W_{pr} used to heat the system at a heating rate β is given by:

$$W_{pr} = \beta C_p \xi + \Delta_r H_T^P \frac{d\xi}{dt} \tag{2}$$

The rate of transformation may be a complex mathematical expression of time and temperature and (or) composition given by the laws of kinetics [7]:

$$\frac{d\xi}{dt} = f(\xi) z \exp - \frac{\Delta H^*}{RT} \tag{3}$$

2.3. DSC

In the case of a heat flow DSC apparatus, the calorimetric signal Δ is given by the temperature difference between the product temperature T_{pr} and that of the reference T_{ref}. It is proportional to the difference between the power absorbed by the product side W_{pr} and the reference side W_{ref}, respectively, $\Delta = k(W_{pr} - W_{ref})$ where k is the sensitivity of the DSC apparatus ($\mu V\ mW^{-1}$)

(α) Constant heating rate: During a temperature scan at a heating rate β, the heat capacity C_{pr} of the sample and C_{ref} of the reference are heated. Then $\Delta = k\beta(C_{pr} - C_{ref})$.

Using Eq. (2), the DSC signal is

$$\frac{\Delta}{k} = \beta(C_{p\xi} - C_{ref}) + \Delta_r H_T^P \frac{d\xi}{dt} \tag{4}$$

Notice that $(C_{p\xi} - C_{ref})$ as written in Eq. (4), is the base line of the DSC.

(β) Non-linear heating rate: A simple model [8,9] of the heat flux DSC is used to describe and understand the behavior of the system.

Step heating [10–12] or periodic [13–16] heating law were described a long time ago, and used in kinetic experiments [17–21] and AC-calorimetry [22–24], respectively.

Recently the idea of using a modulated heating program in DSC, was introduced in a commercially available apparatus [25]. The temperature of the furnace is given by: $T = T_0 + \beta_0 t + A\omega \sin(\omega t)$, where T_0 is the starting temperature, β_0 a constant heating rate, A and $\tau = 2\pi/\omega$ the amplitude and the period of the sine modulation, respectively.

– The signal without sine modulation Δ_{lin} is very close to the same as the signal obtained in linear scanning.
– The amplitude A of the modulation is proportional to $(C_{pr}-C_{ref})$.
– The difference in the phase of the furnace and that of the signal, i.e. the phase shift φ is a complex function, from which C_{pr} can be obtained [26].

If 'true' heat capacity are used, the three curves should have the same or a very similar shape, especially Δ_{lin} and A.

This technic is the subject of a number of papers [26–28], which bring more information on this subject.

3. Experimental

3.1. Material

A DSC apparatus Mettler TA 2000 B was used. It was controlled by a computer [9], which send control parameters to the DSC. It was possible to send to the temperature controller from the computer any heating rate β in the range $\pm 15\ K\ mm^{-1}$. It was found that sending every second the computed rate $\beta=\beta_0+A\omega\cos(\omega t)$ gave the temperature law $T=T_0+\beta_0 t+A\sin(\omega t)$.

A sampling period of 1 s was adequate for the measurement of the calorimetric signal.

The apparatus was flushed with argon chosen on the ground of its density and its low thermal conductivity, which lead to a better calorimetric sensitivity k.

3.2. Products

AC were chosen among SHRP asphalt cements. They contain a low paraffinic content (<0.2%), or a high one (>10%). Pure n-paraffins were purchased from Aldrich.

4. Determination of the thermal properties of AC

4.1. Thermal behavior of asphalt cements

Thermal behavior of Diesel fuels, kerosene, crude oils and bitumen are very similar as shown in Fig. 1. From low to high temperature, a glass transition is observed, followed by two small exothermic peaks and a broad endothermic effect. It is the dissolution of crystallized fractions which precipitated on cooling. Based on this comparison, on warming an AC, the glass transition appears, followed by a small exothermic effect. It is probably linked with the crystallization on warming, of species staying amorphous on cooling. A broad endothermic effect, is then observed. Most often, it occurs under two successive thermal effects, and is due to the dissolution of some CF in the

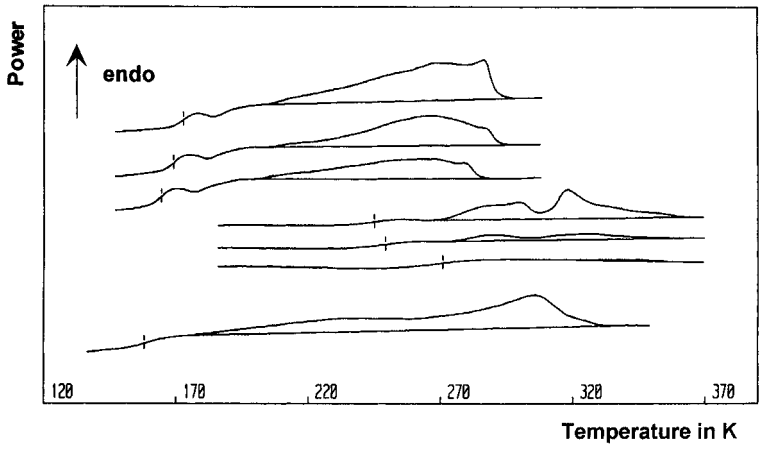

Fig. 1. DSC curves of several petroleum products. From bottom to top: a crude oil; three AC with increasing FC content; and three Diesel fuels. The small line indicates T_g.

liquid formed after the glass transition. The temperature of this minimum is found at ≈35°C.

4.2. Experimental procedure

The thermal properties of AC depend much on their thermal past. Experiments have shown that the sample must have a known and reproducible thermal past so as the DSC experiment can give reproducible results. For this purpose:

(a) The AC is warmed at 100°C during a few hours.
(b) It is cooled at room temperature (25°C), and kept at this temperature during 24 h.
(c) It is put into the DSC and cooled at 10 K mm^{-1} from room temperature to −100°C.
(d) It is warmed at 5 K mm^{-1} up to 100°C, on recording the experiment.

4.3. Glass transition and CF content

The representation of these determinations is given in Fig. 2. The temperature of the glass transition is computed as follows:

(a) Determination of the heat capacities. Heat capacities of the glass $C_{p,glass}$ and of the liquid $C_{p,liq}$ are computed using two points below and two points above the glass transition.
(b) T_g: it is the temperature of the maximum of dC_p/dT.
(c) t_{g1}: it is the temperature of the intersection of the tangent at the maximum of the C_p curve (then at T_g) and the extrapolated curve $C_{p,glass}$.
(d) t_{g2}: it is the temperature of the intersection of the tangent at the maximum of the C_p curve (then at T_g) and the extrapolated curve $C_{p,liq}$.
(e) $T_{g1/2}$: it is the temperature where the heat capacity change is half the total heat capacity change ΔC_p of the glass transition. It is the temperature of intersection of the curve $C_{p1/2}=(C_{p,liq}-C_{p,glass})/2+C_{p,glass}$ with the experimental C_p curve.
(f) ΔC_p: it is the change in heat capacity $\Delta C_p=C_{p,liq}-C_{p,glass}$ at T_g.
(g) CF content: for the computation of the enthalpy change of the dissolution of the crystallized fractions, the base line is shown as a dotted line, which is obtained on drawing the expected heat capacity of the liquid, if no exothermic effect had occurred. The quantity of heat is computed, and transformed in mass of CF, assuming an enthalpy of dissolution of 200 J g^{1}.

5. Dissolution of pure *n*-paraffin in AC

The dissolution of pure *n*-paraffin in an AC having a low content of crystallized fraction was measured. A 3% (wt.) mixture is prepared with the pure *n*-paraffin and the AC, warmed at 100°C, then cured as explained above. Determination of C_p of this mixture is carried out.

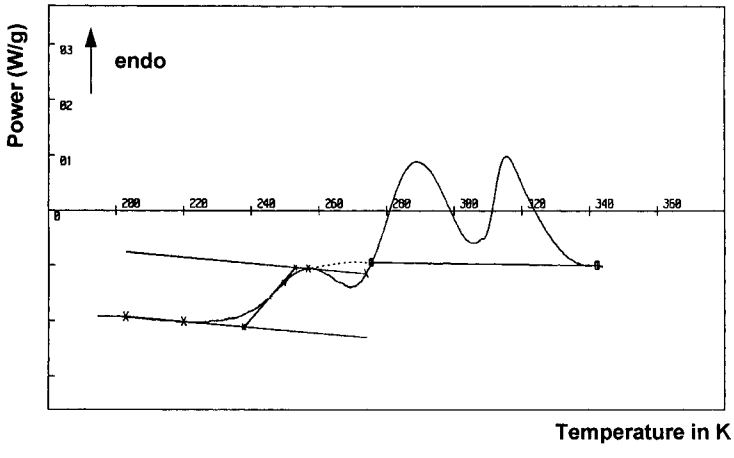

Fig. 2. Example of determination of T_g and FC: x represent the heat capacities of the glass and of the liquid; * the four temperatures of glass transition: t_{g1}, $t_{g1/2}$, T_g, t_{g2}. ○ the base line for FC calculation, – the base line showing the exothermic effect.

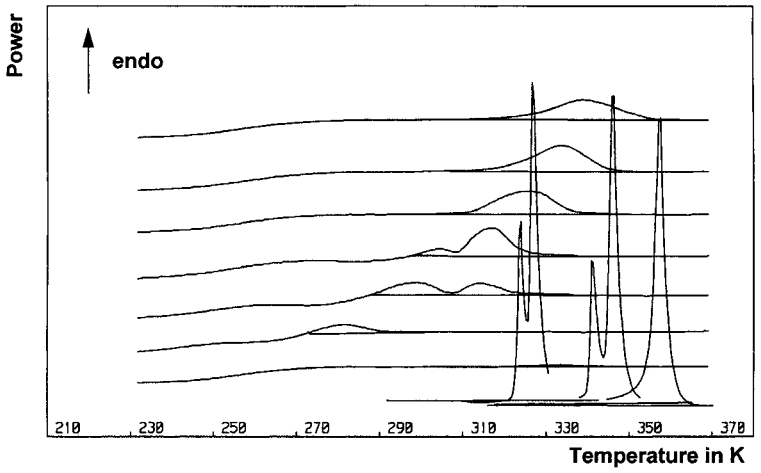

Fig. 3. Dissolution of n paraffins in an AC containing a small mass of CF. From bottom to top: pure AC, C_{20}, C_{24}, C_{28}, C_{32}, C_{36}, C_{40}. The peaks are C_{24}, C_{32} and C_{40}, respectively.

Results are plotted in Fig. 3 for $20 \leq n \leq 40$. As a comparison, the DSC curves of pure C_{24}, C_{32} and C_{40} are given. Clearly, n-paraffins do not 'melt' in the AC, but they dissolve.

(a) The glass transition is always seen, and T_g is slightly lowered for $20 \leq n \leq 32$.
(b) An exothermic effect appears after the glass transition, showing that the crystallization is difficult on cooling.
(c) A broad peak appears, but for C_{24}, and C_{28} it splits into two peaks. The temperature of the minimum called T_{d1} is approximately the same: $T_{d1} \approx 38^{\circ}C$ (see C_{24}, C_{28} and C_{32}).

From these experiments, enthalpy of dissolution is found as 200 J g^{-1} and used to compute the equivalent paraffinic content of the crystallized fraction.

6. Dissolution of n $C_{24}H_{50}$ versus concentration

The dissolution of pure n-paraffin seems to occur in two steps. A more detailed examination of this behavior was required. Experiments are done as explained in Section 4.

6.1. Experiments

The composition dependence on the behavior of C_{24} in AC is given in Fig. 4. The transition-melting curve of pure n $C_{24}H_{50}$ obtained using the same experimental conditions is given for comparison purpose. Below 3% (wt.), only one peak of dissolution is observed. Two peaks are seen at a higher composition. In Fig. 5, the subtraction of the curve $(C_{24}+AC)-(AC)$ is given and the observations made are as follows.

(a) At 0.9%, no signal is seen, the paraffin does not crystallize on cooling or on warming, in the experimental conditions.
(b) The exothermic effect after glass transition, decreases on increasing the composition in C_{24}.
(c) The temperature of the minimum between the peaks T_{d1} stays approximately constant. It is the same as the minimum observed in DSC curve of other AC.
(d) The T_g decreases very slightly, more for low percent of C_{24} than for higher one.

6.2. Discussion

Dissolution of a solid in a liquid is a single curve. (In the case of an ideal solution, the theoretical equation is easily found). Since two peaks are observed, it is believed that a liquid–liquid demixtion occurs, (two liquids are formed) giving rise to two peaks of dissolution. The chemical composition of each liquid is not known.

In fact this explanation is not entirely satisfactory, since the solubility of C_{24} should change with tem-

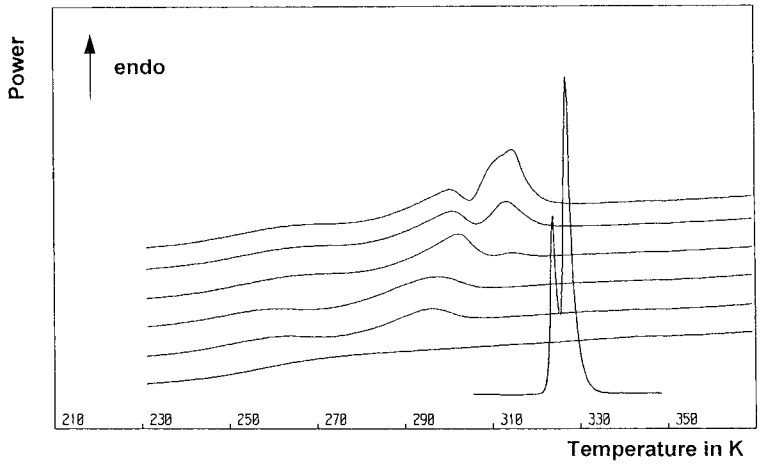

Fig. 4. Dissolution of C_{24} in an AC containing a small mass of CF. C_{24}. From bottom to top: pure AC, and AC with 2, 2.51, 3, 4.03 and 7.01% of C_{24}.

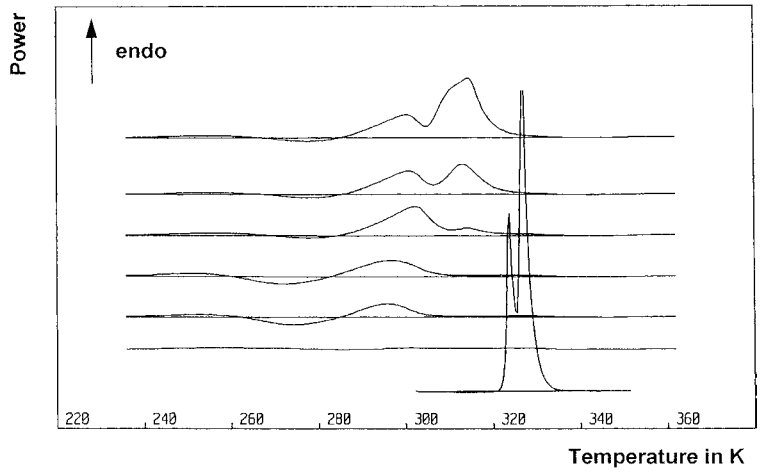

Fig. 5. Subtraction of the DSC curves of AC+n% C_{24} and pure AC.

perature, and it is difficult to explain the observed minimum T_{d1}, excepted if another unknown phenomenon, is occurring.

On cooling, the paraffin should crystallize. But the rate of crystallization depends on the concentration of the paraffin. At low concentrations, it does not crystallize. The composition of the glass formed is not the same as that of the initial glass. Its T_g is lower, because the molecular weight of the paraffin is lower than that of the AC. At a higher concentration, the crystallization is not complete on cooling, giving rise to the exothermic effect observed on cooling, and a weaker influence on T_g. At high concentrations, paraffin crystallizes on cooling, and no effect is observed on T_g, and no without exothermic effect.

Note that this behavior is consistent with the observation of two liquids by thermomicroscopy [29] using Zernick's method.

7. Relaxation experiments

Since bitumen have a glass transition (T) and since the crystallization is difficult on cooling, hence time

(t) and temperature (T) dependent, the time–temperature transformation (t, T, T) of the same AC should be complex and need a reexamination.

7.1. Isochronous experiments

The sample was warmed at 80°C for several hours, then put into an oven at the temperature T. After 24 h, it was put into the DSC at the temperature T or below, and the experiment was done as explained in Section 3.

The behavior of the AC is dramatically changed as shown in Fig. 6

(a) The glass transition easily seen on the +15°C curve is more and more difficult to detect.
(b) The first endothermic peak seems to split into two peaks.
(c) The high temperature peak is not changed.
(d) The total area of the endothermic effect increases, when the storage temperature decreases, suggesting that a larger quantity of crystallized fractions appears.

7.2. Isothermal experiments

The same kind of experiment was done at a constant temperature (−15°C) using different duration. The same kind of conclusion is reached, (see Fig. 7) on changing longer duration for lower temperature.

7.3. Discussion

As expected, the changes occurring in the sample are due to the enthalpic relaxation of glass, to a change in their composition, depending mainly on the temperature, and due to the crystallization.

8. Variable heating rate DSC

A correct interpretation of DSC requires the knowledge of the base line, i.e. the true heat capacity of the sample. An examination of AC samples annealed at −15°C at different duration, was done using a linear heating rate β (3.5 K mn^{-1}) plus a sine modulation (amplitude 1 K, period 2 mn).

8.1. Computation

The calorimetric signal is given by Eq. (4). Since the frequency of the temperature modulation is known, it is fitted by a least-squares method [30] to the equation:

$$\Delta = A_1 \sin(\omega t) + A_2 \cos(\omega t) + Bt + T_0. \quad (5)$$

The amplitude A of the modulation is given by

$$A = \sqrt{A_1^2 + A_2^2} \quad (6)$$

and its phase shift φ is given by:

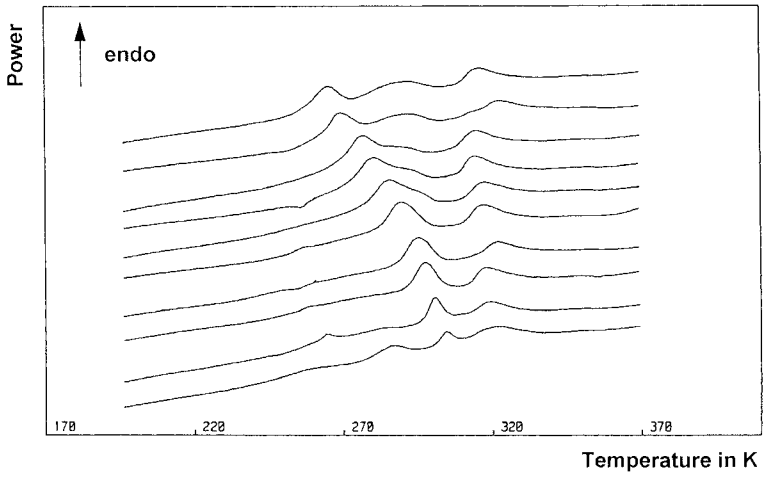

Fig. 6. DSC curves of an AC kept 24 h at the temperature T. From top to bottom: −30°, −25°, −20°, −15°, −10°, −5°, 0°, 5°, 10°, 15°C.

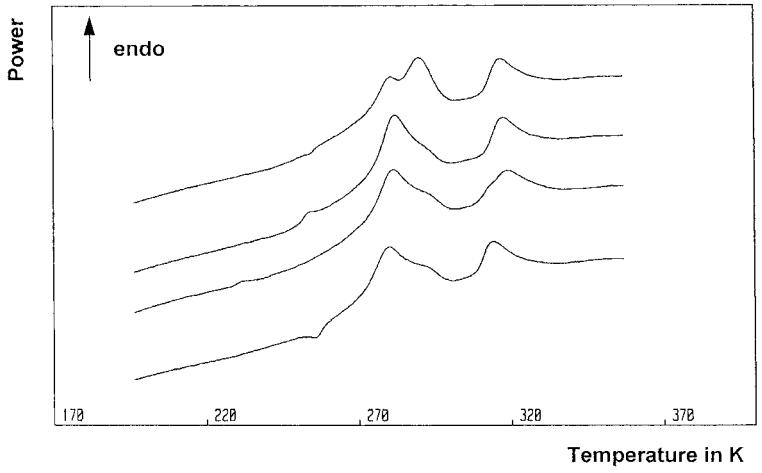

Fig. 7. DSC curves of an AC kept at −10°C at different times. From bottom to top: 1, 2, 4, 8 days.

$$Tg(\varphi) = \frac{A_1}{A_2}. \quad (7)$$

Measurements used for each computation are those done during half of a period. The data at $t_1, t_2, \ldots t_n$ are used to compute A_1, A_2, A and φ at time $t_n - t_1/2$ using Eqs. (5)–(7), respectively. The values at t_2, $t_3 \ldots t_{n+1}$ give A and φ at time $t_{n+1} - t_2/2$ and so on.

The signal without modulation is obtained from

$$\Delta_A = Bt + \Delta_0 \quad (8)$$

8.2. Standardization

The standardization of the DSC is done using 'true' heat capacities, namely several masses of aluminum.

Three curves, and three determinations of the heat capacity of the sample, are obtained for each experiment:

(a) using the average signal Δ_A;
(b) using the amplitude A; and
(c) using the phase shift T_g φ.

Heat capacity is obtained by interpolation, using the standardization curves obtained with several masses of pure aluminum.

8.3. Results

8.3.1. Diesel fuel

Since the rate of transformation is much faster on a sample having a low viscosity, it was interesting to test the method of calculation developed above on a Diesel fuel. An experiment is shown in Fig. 8. The glass transition is observed followed by two effects seen on the average signal and not on the amplitude or phase shift. This means that these effects do not depend on the temperature, but only on the time. Then they are crystallization effects. The endothermic effect seen at a higher temperature is the dissolution of the CF (paraffin), and is seen on the three curves at high temperature meaning that the rate of dissolution is high. It is not possible using a 2 mn period, to distinguish between C_p and $C_{p\xi}$. These results are consistent with those of Sanier [31].

8.3.2. Asphalt cement

(α) Sample annealed at −10°C: Examination of a sample annealed at −10°C during several duration was done using modulated DSC. The difference between the apparent heat capacity (C_p) and the true heat capacity ($C_{p\xi}$ at low temperature) as reported in Fig. 9, shows:

– the separation between the curves C_p and $C_{p\xi}$ occurs at the relaxation temperature;
– a glass is formed with a T_g at ≈17°C as measured on the $C_{p\xi}$ curve, its quantity depending on the duration
– T_g is difficult to establish, using either curve.

(β) Sample annealed at −30°C: Experiments are given in Fig. 10. The same observations as in the experiment at −10°C are valid, excepted that a new peak

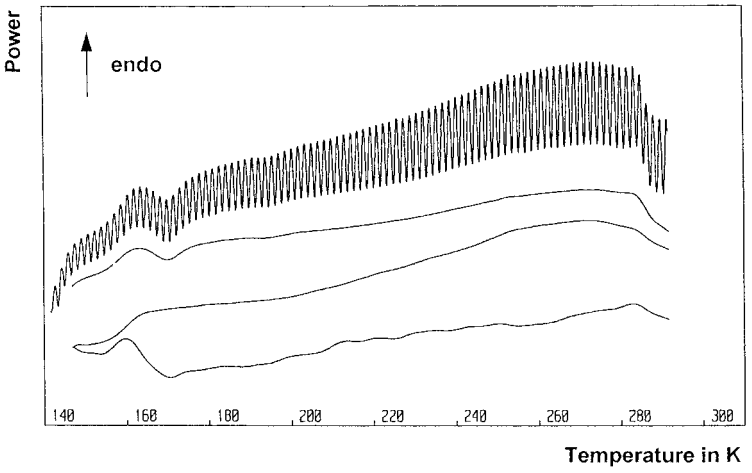

Fig. 8. Modulated DSC curve of a Diesel fuel. From bottom to top: heat capacities computed from phase shift φ, amplitude, average signal, and the raw experiment.

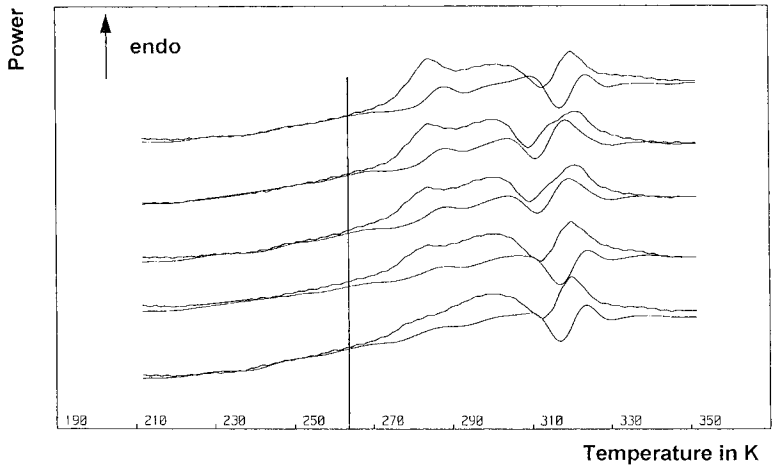

Fig. 9. Modulated DSC curve of an AC kept at −10°C. Each couple of curve shows the heat capacities computed from amplitude (below) and average signal. From bottom to top times were 1, 2, 4, 8, 16 h. The vertical line shows the relaxation temperature (−10°C).

appears, at low temperature. After this peak, an exothermic effect appears. It decreases at longer duration.

In Fig. 11 a closer examination of the three curves (average, amplitude, phase shift) seems to show two glass transitions appearing on the sample annealed at −30°C during 16 h.

8.3.3. Discussion

The AC used contains a large amount of crystallized fraction, and two liquids at room temperature. On cooling, these two liquids may give two glasses one with a high T_g, and the other with a low one, at least below −10°C. Depending on the time, the CF can crystallize, and probably, change the respective quantities of each glass, and even their T_g, as seen in Section 5.

At −30°C, both liquids have been transformed into glasses, whose glass transition are seen. These glasses show the well-known enthalpic relaxation peak [32,33] seen at low temperature.

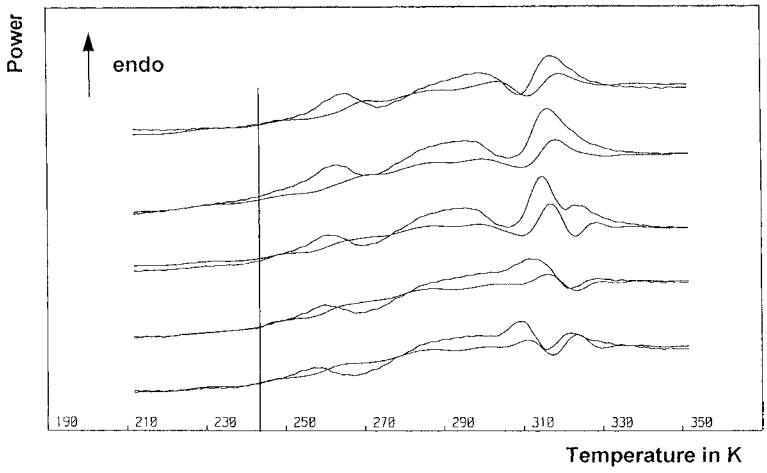

Fig. 10. Modulated DSC curve of an AC kept at −30°C. Each couple of curve shows the heat capacities computed from amplitude (below) and average signal. From bottom to top times were 1, 2, 4, 8, 16 h. The vertical line shows the relaxation temperature (−30°C).

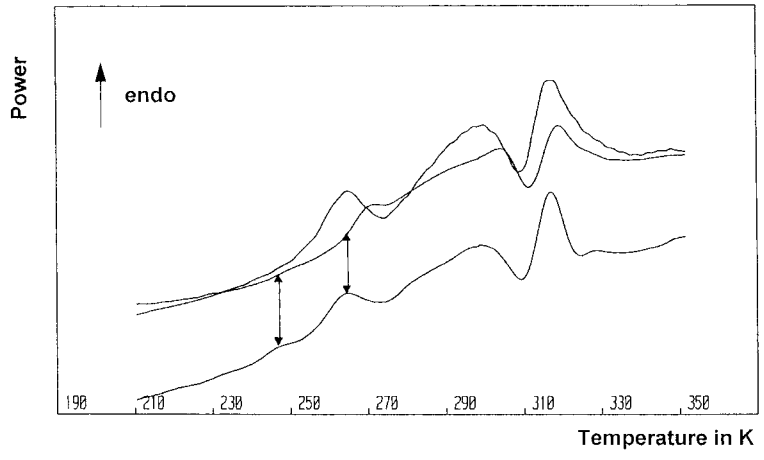

Fig. 11. Modulated DSC curve of an AC kept at −30°C during 16 h. showing two glass transitions indicated by an arrow. the three curves are the heat capacities computed from phase shift (below), amplitude (middle) and average signal (top).

9. Conclusion

At room temperature, an AC is made of two liquids, and some crystallized fractions. On cooling, simple but intricate phenomenons occur.

The quantity of CF increases, because their solubility decreases with temperature, but not enough to prevent the formation of two liquids. These liquids give one or two glasses, depending on the temperature.

The double glass transition seems to be a natural consequence of the liquid–liquid demixtion occurring in an AC, each liquid giving a glass. The proportion of each glass should vary, depending on the thermal history of the sample. That could explain the very broad temperature range of the glass transition, and the very complex behavior of the relaxation of the AC.

The rate at which the equilibrium is reached, is certainly very low, and mechanical properties may change on a very long period, since mechanical properties of an AC are a consequence of the nature of the phases formed.

References

[1] C.J. Mack, Bituminous Materials, Asphalts, Tars and Pitches, In: A.J. Hoïberg (Ed.), Interscience, New York, 1 (1964) 25.
[2] H.J. Connor, J.G. Spiro, J. Inst. Petrol. 54 (1968) 533.
[3] F. Noël, L.W. Corbett, J. Inst. Petrol. 56 (1970) 551.
[4] M. Albert, F. Bosselet, P. Claudy, J.M. Létoffé, E. Lopez, B. Damin, B. Neff, Thermochim. Acta 84 (1985) 101–110.
[5] D.A. Anderson, D.W. Christensen, J. of Assoc. of Asphalt Paving Technologists 61 (1992).
[6] I. Prigogine, R. Defay, Thermodynamique Chimique. Desoer Ed., Liège (1950).
[7] J. Sestak, V. Sastava, W.W. Wendlandt, Review: The study of heterogeneous processes by thermal analysis, Thermochim. Acta 7 (1974) 333.
[8] I. Hatta, H. Ikushima, Jpn. J. Appl. Phys. 20 (1981) 1995.
[9] P. Claudy, J.C. Commerçon, J.M. Létoffé, Thermochim. Acta 65 (1983) 45.
[10] J. Synger, Anal. Chem. 47 (1975) 1380–1384.
[11] K.A. Simonsen, M. Zaharescu, J. Therm. Analysis. 15 (1979) 25–35.
[12] P. Claudy, J.C. Commerçon, J.M. Létoffé, Thermochim. Acta. 128 (1988) 251–260.
[13] I. Proks, I. Zlatovsky, Chem. Zvesti 23 (1969) 620–632.
[14] I. Proks, I. Zlatovsky, K. Adamkovicova, Davos, August 23–28, (1971) Abstract I–44.
[15] N.O. Birge, S.R. Nagel, Phys. Rev. Lett. 54 (1985) 2674–2677.
[16] M. Massalska-Arodz, Phys. Rev. B 43(16) (1991) 1366–1378.
[17] J.H. Swinehart, J. Chem. Ed. 9 (1967) 524–526.
[18] J.E. Finholt, J. Chem. Ed. 6 (1968) 394–397.
[19] H. Winkler, Endeavor 33(119) (1974) 73–79.
[20] A. Zuda, Thermochim. Acta 8 (1974) 217–219.
[21] J.A. Azizi, D. Dollimore, G.R. Heal, P. Manley, W.A. Kellner, W. Jin Yong, J. Thermal Anal. 40 (1992) 831.
[22] Ya.A. Kraftmakher, Zh. Prikl. Mekhan Tekhn. Fiz. 5 (1967) 176.
[23] N.O. Birge, S.R. Nagel, Phys. Rev. Lett. 54 (1985) 2674–2677.
[24] Y.A. Kraftmakher, Modulation calorimetry in Compendium of thermophysical property measurement methods. K.D. Maglic, A. Cezairliyan, V.E. Pemetsky (eds) Vol. 1 Plenum Press 1984, Chap. 15 pp 592–639.
[25] M. Reading, B. Crowe, B.K. Hahn, US patent 5224775, July 6, 1993.
[26] P. Claudy, J.M. Létoffé, J. Therm. Analysis to be published.
[27] B. Wunderlich, J. Thermal. Anal., 48 (1997) 207–224; B. Wunderlich, Y. Jin, A. Boller, Thermochim. Acta 238 (1994) 277–293.
[28] A.A. Lacey, C. Nikolopoulos, M. Reading, J. Thermal. Anal. 50 (1997) 279–333.
[29] P. Claudy, J.M. Létoffé, J.P. Planche, G.N. King, International Symposium Chemistry of Bitumen, ROME 5–7 July 1991.
[30] B.J. Frohring, B.E. Peetz, M.A. Unkirch, S.C. Bird, Hewlett Packard Journal 39 (1988) 39.
[31] A. Zanier, H.W. Jäckle, Thermochim. Acta 287 (1996) 203–212.
[32] S.V. Nemilov, Thermodynamic and kinetic aspects of the vitreous state. CRC Press, Boca Raton, Ann Arbor, London, Tokyo 1995.
[33] J. Zarzycki, Les verres et l'état vitreux, Masson Ed., Paris 1982.